Quantitative Attachment and Detachment of Bacterial Spores from Fine Wires through Continuous and Pulsed DC Electrophoretic Deposition

Wenbo Zhou,[†] Sarah K. Watt,[‡] De-Hao Tsai,[†] Vincent T. Lee,*,[‡] and Michael R. Zachariah*,[†]

[†]Department of Chemistry and Biochemistry and Department of Mechanical Engineering, [‡]Department of Cell Biology & Molecular Genetics, University of Maryland, College Park, Maryland 20742, United States

🅢 *Supporting Information*

ABSTRACT: We demonstrate the uniform attachment of bacterial spores electrophoretically onto fine wires in liquids and subsequently quantitatively detached back into suspension. It was found that the use of a pulsed voltage method resulted in a uniform coverage of spores and prevented visible bubble formation resulting from water electrolysis which tended to dislodge the spores from the wires. By monitoring the electrophoretically derived current, this method could also be used to quantitatively measure the surface charges on spores and the deposition rate. The method is generic and should be applicable to the deposition of any charged biological material (e.g., spores, bacteria, viruses) onto metal surfaces.
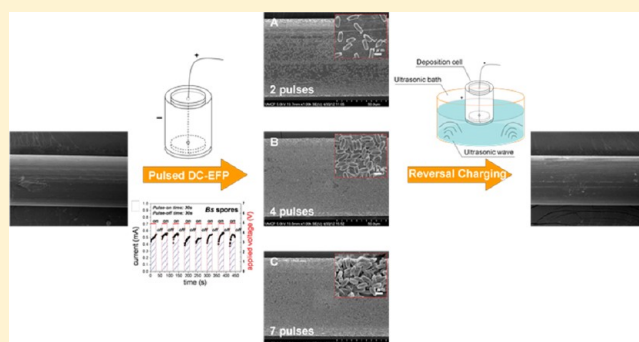
1. INTRODUCTION

Concerns on bioterrorism[1,2] have prompted efforts to discover, quantify, and compare neutralization methods such as heat,[3,4] chemical,[5] and other synergistic effects.[6−8] The extreme stress-resistance of bacterial spores[9] has provided the impetus to develop quantitative studies to more precisely define various neutralization mechanisms. Previous studies in defining spore neutralization have focused on heating under 100 °C in the absence of pressure or the combination of heat and pressure with inactivation time scale in the order of minutes.[10,11] In particular, a temperature−time relationship for spore inactivation for high temperatures (100−1000 °C) and short times (10 ms to 10 s) is still not available. The first approach to address this problem is to initiate thermal reactions in sealed chambers in which the temperature between 200 and 700 °C is monitored and correlated with the number of recovered viable spores.[4,12,13] These experiments are limited by the ability to precisely manipulate the temperature and exposure time. Another approach recently employed has been to disperse spores in the aerosol phase and subject them to high temperatures between ∼150 and >1000 °C and chemical environments.[3,14] However, there exists a temperature distribution in the aerosol flow in these studies, which causes a decrease in the precision of the temperature−viability relationship. A third approach is to immobilize spores on a surface that can be thermally varied in a precise manner. This approach can cover a larger temperature range[15] in short time scales and allows convenient enumeration of viable spores immediately after thermal exposure.

The latter method is only useful if a well-defined spore population can be coated on the surface. Typically, this might be accomplished in a liquid suspension either naturally[16−18] or by laboratory manipulation.[19,20] Bacteria naturally have various adhesins to promote attachment to plastic, glass, and metal surfaces to form biofilms.[16−18] In the laboratory, poly-L-lysine can be coated to impart a net positive charge on the surface to promote electrostatic interaction with the negatively charged exterior of most bacteria. However, neither mechanism can be utilized for the studies of spores, as spores are biological inert and often fail to attach to poly-L-lysine coated surfaces.[21] We sought to develop an alternative approach to attach spores onto wires using physical forces.

Previously, dielectrophoresis has been utilized in the manipulation of bacterial spores.[22] In the presence of an electric field gradient, a net force is imparted on the spore due to polarization, the magnitude of which is highly dependent on the material properties of the spore (including size),[23] the characteristics of the fluid (including ionic strength and dielectric permittivity of the solvent and solute),[24] and the field gradient.[25−28] Dielectrophoresis is contrasted with electrophoresis which can take place if the cell has a net charge, and is directly proportional to the magnitude of the field.[29,30] Most reported studies however modeled spore transport in liquids as

being net neutral in charge, and only considered the dielectrophoretic effect.[31−33] Actually, in aqueous dispersions, the glycoproteins and polysaccharides that comprise the exosporium (i.e., outer layer) are negatively charged. These negative charges arise from deprotonation of aldehydes (−RCOH), phosphodiester (−(RO)$_2$POOH), and carboxylic acids (−RCOOH), which have been detected by the infrared spectroscopy[34] and zeta potential analysis.[35]

Electrophoretic deposition (EPD) has been used in the past for a wide variety of bioparticles including bacteria,[36,37] protein inclusion bodies,[38] and yeast cells.[39] While the generic process of EPD of bioparticles is similar, the exact rates of attachment to the wire may be complicated by side effects including bubble formation,[40,41] surface chemistry,[42,43] electrode curvature effects,[44] and excretion of adhesive extracellular media[45,46] Bubble formation appears to be a significant problem for controlled and effective EPD. Two approaches have been reported to minimize this effect. AC-EPD has been found as a powerful method to mitigate the water electrolysis under some frequency conditions.[47,48] Pulsed DC-EPD has also been shown to obtain dense bubble-free deposits at suitable pulse widths and duty cycles.[49,50] From a practical standpoint, pulsed DC-EPD is a simpler approach that is easier to implement.

Besides the electrostatic interaction forces and the bubble formation effects on attachment, other forces may also contribute to the attachment of spores to surfaces. The Lifshitz−van der Waals force between the spore surface and the electrode surface can be described by the well-known Derjaguin−Landau−Verwey−Overbeek (DLVO) theory.[51] The image force which arises due to the induced dipole effect between the charged spore and the surface can also influence deposition and has been detected by atomic force microscopy.[52] While the Lifshitz−van der Waals force, the image force, and the electrostatic force all have an inverse square distance relationship, for the problem under consideration here, it has been shown that the dominant effect can be attributed to the electrostatic force.[53]

In this study, we will investigate electrophoretic attachment of uniform layers of spores to fine wires, and demonstrate reversible detachment. We demonstrate that, by applying a pulsed direct current (DC), we can quantify incremental spore attachment with time by measuring the electrical current to the wire electrode. The advantages of this charging mode will be shown over the continuous charging mode. By using the measured current which can be directly related to the spore flux to the surface, we are further able to validate a transport model and use the model to directly determine the average spore surface charge and spore deposition efficiency. This methodology developed here is to our knowledge the first demonstration of direct quantitative attachment and detachment of spores from fine wires.

2. EXPERIMENTAL APPROACH TO SPORE ATTACHMENT AND DETACHMENT

2.1. Spore Deposition Cell.
The spore deposition cell is shown schematically in Figure 1. It is composed of four compartments: an outer PTFE tubular shell with sealed base, a stainless steel cylinder as the outer electrode, a central wire as the deposition surface and inner electrode, and two PTFE plates to center the wire. The stainless steel outer electrode has an inner diameter of 16 mm and a height of 20 mm. For the wire central deposition electrode, we use 76.2 μm platinum (Pt) (Omega Engineering, Inc.), since it is very stable in
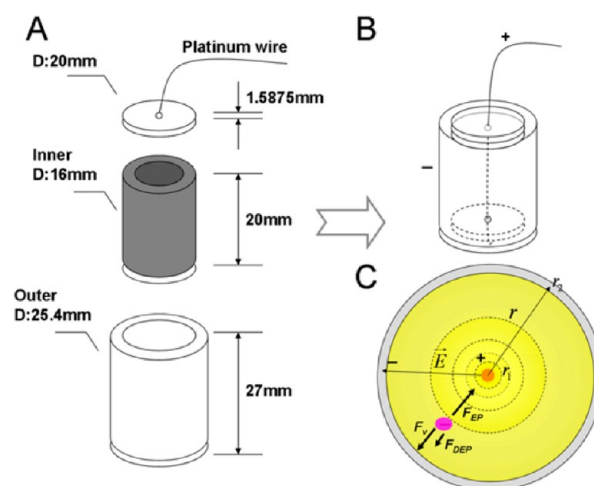
Figure 1. (A) Components of the spore deposition cell which includes an outer protection cylindrical shell, an inner stainless steel tube, two PTFE center-pierced plates, and the central wire. (B) Assembled cell in the spore coating process, with the wire as the anode and the stainless steel tube as the cathode. Part C shows the electric field distribution between two electrodes and the forces that the negatively charged spores experience in the liquid phase.

aqueous systems and will not be oxidized. The spore strain adopted in these studies is *Bacillus subtilis* (*Bs*) spores ATCC#6051 (see the optical microscopic image in Figure S1, Supporting Information), which were sporulated by growth in Difco Sporulation Medium (DSM) at 30 °C for 48 h. A 250 mL DSM was prepared which included 2 g of Bacto nutrient broth, 2.5 mL of 10% KCl, 0.375 mL of 1 M NaOH, and 2.5 mL of 1.2% MgSO$_4$·7H$_2$O. The initial spore number concentration was regulated to be 8×10^9 CFU/mL.

The power supply and current detection were performed with a 6430 sub-femtoamp remote sourcemeter from Keithley. Ultrasonication employed a Branson model 5510 ultrasonic cleaner. Optical microscopic images were taken by a Zeiss AxioObserver microscrope using a 40× objective with phase contrast illumination. Scanning electronic microscopic (SEM) images were taken of spores on wires fixed with 2% glutaldehyde, dehydrated through a series of alcohol, and sputter coated with platinum. Images were captured with a Hitachi S4700 FESEM in the Laboratory of Biological Ultrastructure at the University of Maryland. To validate our spore charging measurement approach, we employed zeta-potential analyses from a Zetasizer Nano ZS (Malvern Instruments, U.K.) equipped with a 633 nm laser and a palladium dip cell module. A 500 μL portion of sample suspension was mixed with 250 μL of 10 mM ammonium acetate aqueous solution prior to the measurement.

2.2. Spore Attachment in Continuous and Pulsed DC Charging Modes.
The fine wire was stabilized inside the spore deposition cell vertically, and the spore suspension was added into the cell to immerse the wire up to a depth of 1 cm. The central wire was connected with the positive pole of the power supply, and the outer stainless steel cylinder was connected to the negative pole. A variety of EPD measurements were performed with varying voltages and on-times, and real-time current data were stored. Comparably, fine wires with different compositions and diameters were tested to find an optimal one. In the pulsed DC charging mode, a series of pulsed on-times and off-times were controlled to differentiate

from the continuous charging mode, and the optimal pulsed charging condition for *Bs* spores ATCC#6051 was found.

2.3. Optical Microscopic and SEM Analyses. Wires coated with spores were observed under optical microscopy over glass slides and also by the naked eye. For the SEM analyses, samples were first fixed in 2% glutaraldehyde in buffer for 1 h at room temperature. Excess glutaraldehyde was removed in buffer by three washes of 10 min each. The samples were post fixed with 1−2% osmium tetroxide in the above buffer for at least 30 min, and then with double distilled water. After a series of dehydration processes in ethanol, the samples were treated with critical point drying with liquid carbon dioxide. Finally, samples were mounted to stubs and coated with gold/palladium alloy.

2.4. Spore Detachment. A very important aspect of this work was to develop the methodology to detach spores from the wire. To accomplish this, the wire loaded with spores was placed in a clean cell with distilled water and the wire oppositely biased to be the cathode. Simultaneously, the cell was immersed into an ultrasonic bath. The separate effects of opposite biasing and ultrasonication were compared. The detached spores were harvested for spore plate counting, as will be shown later. The treated wire was inspected by optical microscopic and SEM analyses to find if all the attached spores were removed from the surface.

2.5. Spore Plate Counting Assay. Spores detached from wires were counted by enumerating colony forming units (CFU) by plating serial dilutions on LB agar plates. Counting was repeated four times, and an averaged value was reported.

3. SPORE TRANSPORT MODEL

The use of the cylindrical deposition cell geometry enabled quantitative modeling, since the electric field is well described as

$$|\vec{E}| = \frac{\Delta U}{r \ln \frac{r_2}{r_1}} \tag{1}$$

where ΔU is the voltage difference between two electrodes, r is the radical distance from the center, and r_1 and r_2 are the diameters of the inner (wire) and outer cylindrical electrodes. In our design, $r_1 = 0.0381$ mm and $r_2 = 8$ mm. It is well-known that spores when introduced into an aqueous medium will acquire a net charge[34,35] and thus can be manipulated with an electric field. The electrophoretic force on a spore with q charges in an applied electric field is

$$F_{EP} = qE \tag{2}$$

The presence of the field will also induce polarization within the spore, which if the field is spatially invariant will impart no net force on the spore. However, in the presence of an electric field gradient, the spore will also experience a net dielectrophoretic force:[22]

$$F_{DEP} = 2\pi\varepsilon_m R^3 \, \text{Re}(f)\nabla E^2 \tag{3}$$

where ε_m is the permittivity of the surrounding water (7.1×10^{-10} F/m) at room temperature, R is the radius of the spore, and Re(f) is the real part of the Clausius−Mossotti factor. In a DC field, this factor is directly related to the conductance of both the spore surface and the media:[22]

$$\text{Re}(f) = \frac{\sigma_p - \sigma_m}{\sigma_p + 2\sigma_m} \tag{4}$$

Herein, σ_p and σ_m stand for the conductivities of spores and media. At room temperature, σ_p is 10^{-7} S/m (as the cell membrane[54]) and σ_m is 5.5×10^{-6} S/m. Hence, Re(f) is a negative value which implies that the direction of F_{DEP} is opposite to the direction of F_{EP}, as in Figure 1C. Meanwhile, the retarding force is caused by the viscous drag and can be evaluated with Stoke's law:

$$F_v = -6\eta\pi R u \tag{5}$$

where η is the viscosity of water (1.002×10^{-3} Pa·s) at room temperature and u is the velocity of spores. It should be noted that the *Bs* spores are not strictly spherical; thus, R in both eqs 3 and 5 is an effective radius (a spherical spore with this effective radius is defined to have the same volume as a real spore). From previous reports of spore volumes,[55] the effective R value for *Bs* spores is 0.336 μm. The spore motion can then be directly evaluated in a force balance:

$$\Delta F = m_s \frac{d^2 r}{dt^2} = F_{DEP} + F_{EP} + F_v \tag{6}$$

Since the inertia term is relatively small (i.e., the spore response time to any voltage perturbation is fast relative to the transit time), we can assume steady state ($\Delta F = 0$). The resulting governing equation becomes

$$\frac{dr}{dt} = \frac{A}{r} + \frac{B}{r^3} \tag{7}$$

where $A = \Delta U \cdot q/(0.101R)$, $B = 8.26 \times 10^{-9}(\Delta U)^2 R^2$.

The above equation describes the spore velocity at any radial location in the cell between two cylindrical electrodes and thus can be directly related to the experimental current data, since it is the motion of spores that contributes to the current formation. The time for spores with an initial distance $r + \Delta r$ away from the center to move a differential distance of Δr is from eq 7:

$$\Delta t = \frac{r^2 - (r + \Delta r)^2}{2A} + \frac{B}{2A^2} \ln \frac{A^2(r + \Delta r)^2 + AB}{A^2 r^2 + AB} \tag{8}$$

In this time interval, the total charge quantity passing through this differential distance Δr is

$$\Delta Q = q'C\Delta V = q'C\pi l[(r + \Delta r)^2 - r^2] \tag{9}$$

where C is the spore number concentration in the cell, l is the immersed depth of Pt wire inside the liquid (0.01m), and ΔV is the differential volume element around the wire. It should be noted that the charge q' is the effective overall charge after being shielded by counterions in the vicinity of the spore surface (i.e., the diffuse double layer). The importance of this is that the mobility of a spore is influenced by the thickness of the double layer that is dragged along with the spore. The current can be expressed as

$$I = \lim_{\Delta t \to 0} \left| \frac{\Delta Q}{\Delta t} \right| = \frac{2q'\pi Cl(Ar^2 + B)}{r^2} \tag{10}$$

Then, substituting for A and B above, the initial current observed can be expressed as

$$I_0 = \frac{0.622C\Delta U}{R}q'q + 3.58 \times 10^{-7}C\Delta U^2 R^2 q' \tag{11}$$

Equation 11 is a simplified illustration of the current corresponding to the spore deposition rate but which does
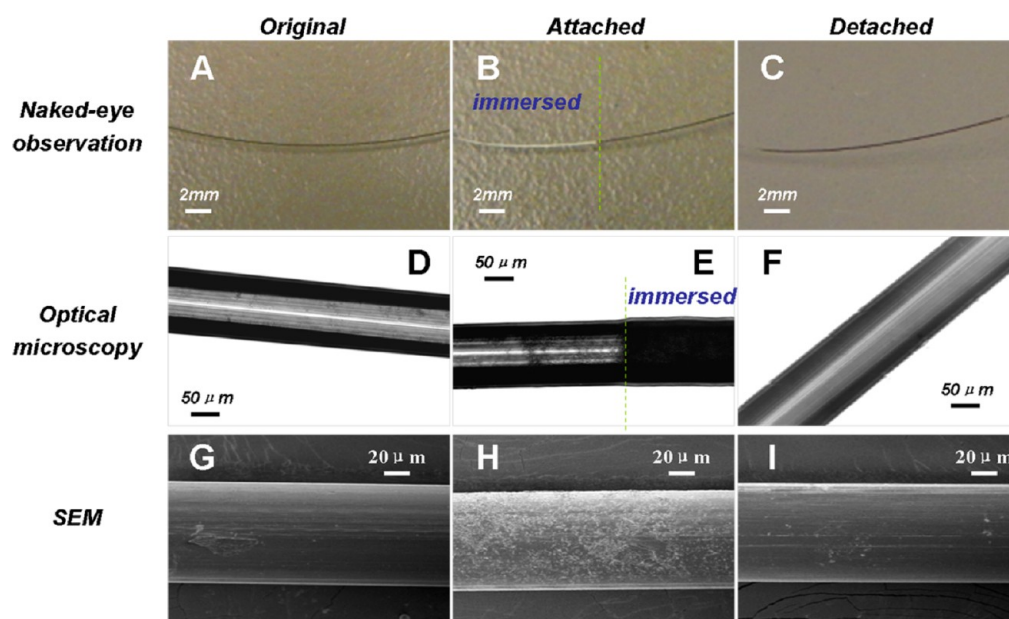
Figure 2. Parts A−C show Pt wires before coating, after coating, and after detaching. Parts D−F show optical microscopic images of Pt wires before coating, after coating, and after detaching. In both parts B and E, the immersed parts of the wire inside the spore suspension were marked. Parts G−I show SEM images of Pt wires before coating, after coating, and after detaching. The charging condition for spore attachment is 20 s at 20 V. The spore detaching condition is 10−15 min at reversed 60 V, combined with the ultrasonication.

not include possible effects due to particle−particle and particle−electrode interactions. Near the electrode, the spore transport may be complicated by electrohydrodynamic flows as well as electroosmotic flows due to the electric forces on charges from the electrode polarization layer and the equilibrium diffuse double layer near the spore.[56,57] However, since eq 11 describes the initial current when $t = 0$, the influence of those flows can be neglected. In the remainder of the paper, we analyze our experimental results in the context of the model resulting in eq 11.

4. RESULTS AND DISCUSSION

4.1. Spore Attachment in the Continuous DC Mode. To exemplify the spore attachment in the continuous DC mode, a biased voltage of 20 V and a spore number concentration of 8×10^9 CFU/mL were adopted. The EPD conditions employed were chosen on the basis of prior work that showed that bacterial spores can withstand DC electric fields as high as 1500 V/cm and still maintain viability.[31] Before we proceeded with direct measurement of the current in evaluating spore deposition, we evaluated the temporal variation of current for pure water and the spore suspension in Figure S2 (Supporting Information). We found that steady state could be achieved on the order of 100 s, and that the measured current due to charge migration in the spore containing suspension was about an order of magnitude larger than that contributed to by pure water. This allows us to ignore the influence of the solvent in subsequent current measurements during EPD. Images of spore attachment are shown in Figure 2 for a deposition time of 20 s. The visual images (Figure 2A and B) show that, after DC biasing, an obvious white spore coating appeared in the immersed portion of the wire. Further optical microscopic images (Figure 2D and E) reflect the spore deposition in that region (the dark region represented the coverage of spores). SEM images (Figure 2G and H) show an evenly distributed and dense coating on the

wire and more directly demonstrated the attachment of spores. The enlarged SEM images in Figure 3A and B also exhibit the structures of attached *Bs* spores on surfaces.
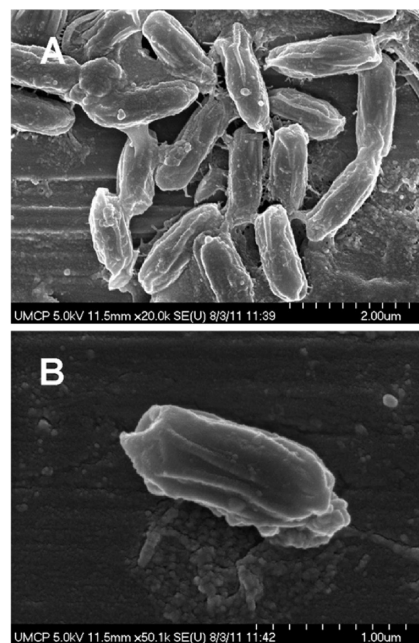
Figure 3. SEM images of *Bs* spores ATCC#6051 attached on Pt wires.

Nominally, we should expect that increasing the charging time would cause incremental increases in spore deposition to the surface. However, such a relationship was not linear especially after a relatively long time, and when a higher voltage was applied (Figure S3, Supporting Information). In those cases, the current−time curves show fluctuations which could be correlated to the generation of visible gas bubbles formed from water electrolysis[58] (Figure S4C, Supporting Informa-

1741

dx.doi.org/10.1021/jp307282q | J. Phys. Chem. B 2013, 117, 1738−1745

tion). As a result, spore deposits became highly uneven along the wire surface, and subsequently were detached from the wire at high voltages, or long charging times (Figure S4A and B, Supporting Information). This prompted us to evaluate a pulsed deposition mode that will be described later.

4.2. Spore Detachment. To properly evaluate our eventual exposure studies (heat, chemicals), an efficient and quantitative method to detach the spores is necessary so that standard assays can be employed. We found that either reversed biasing the wire at −60 V for 5 min or ultrasonicating for 30 min allowed partial detachment of spores from the wire (Figure S5, Supporting Information). While some reports indicate that ultrasonication is known to harm spores[59,60] and repeated electric pulse cycling can also induce spore inactivation,[61,62] we operated at much shorter ultrasonication time and bias voltage which are ~100× less than those studies. Similarly, pH changes which occur during deposition (Figure S6, Supporting Information) were evaluated for viability by exposing spores to a range of pH (5−10) (Figure S7, Supporting Information) and were found to have no effect. We found that the combination of reverse bias and ultrsonication would detach the spores completely.

The photographic, optical microscopic, and SEM images shown in Figure 2C, F, and I, respectively, demonstrate that all the *Bs* spores were removed from the surface after reversed biasing for 10−15 min at −60 V in an ultrasonic bath. Once the spores on the surface were removed into liquid, they could be enumerated by the plate counting method to determine the number of spores deposited on the wire. It should be noted that the reverse-bias charging time and voltage here are larger than those for spore attachment, which presumably accounts for the force required to overcome the binding energy between the spore and wire surface. Together, these results indicate that the combination of reversed biasing and ultrasonication is an effective means to completely remove spores deposited on the surface.

4.3. Spore Attachment in the Pulsed DC Mode. The fluctuation in the deposition current observed (Figure S3, Supporting Information) coincided with visible bubble formation (Figure S4C, Supporting Information). To mitigate this effect, we shifted our efforts to a pulsed DC mode, based on results of Besra et al.[50] who showed that, using a pulsed voltage strategy, an extension of an application used to deposit metal films could lead to a minimization of bubble formation and conformal deposits of small particles. We have adopted this strategy in order to generate a uniform and densely packed spore coating, by applying multiple electric pulses instead of a continuous DC bias. We have found that this leads to reproducible spore deposits by enabling consistent current measurements. In Figure 4, the measured temporal currents during deposition of *Bs* spores (ATCC#6051) at a voltage of 5 V are shown, with an on-time of 30 s followed by an off-time of 30 s. Over eight cycles of this experiment, the measured current was consistent between cycles, which implies that the ionic strength of the liquid was stable. The SEM images (Figure 5) reflect the increase of *Bs* spore attachment on the surface with the pulse number. After charging for two pulses, only partial coverage was achieved; however, these deposits were uniform. A monolayer of *Bs* spores could be formed after four pulses, and multiple layers of spores were found after seven pulses. Optical microscopic images (Figure S8, Supporting Information) also show that the *Bs* spore deposits increased as the pulses accumulated. After enumerating all the spores detached
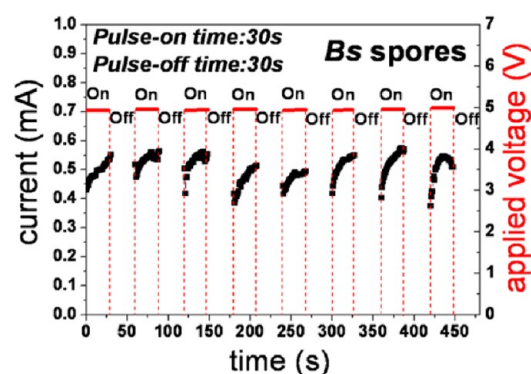
Figure 4. Current−time relationship in the pulsed DC charging mode for *Bs* spores (ATCC#6051). Both the charging time and the pulse-off time were 30 s, and the applied on-time voltage was 5 V. In our design, *Bs* spores were deposited to the surface for up to eight cycles.
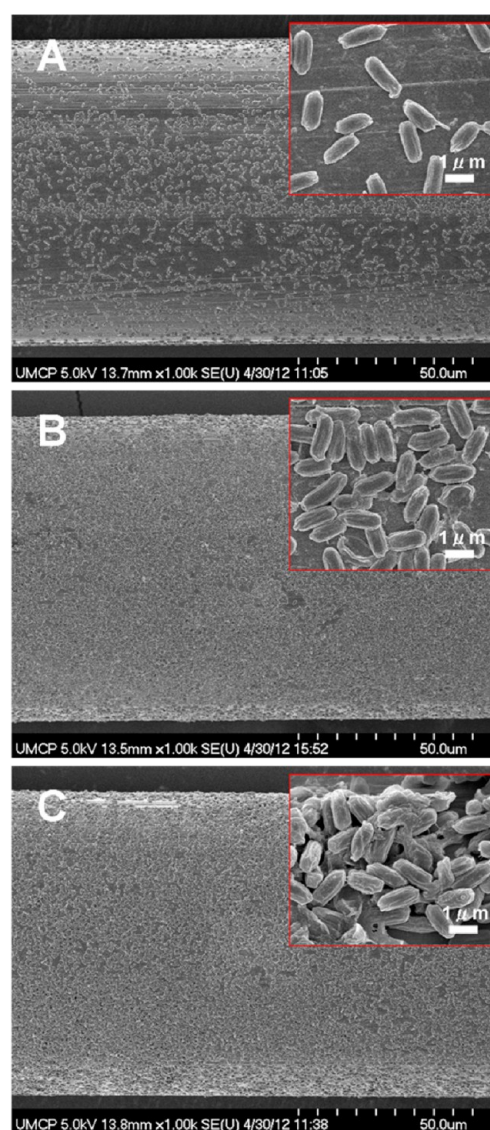
Figure 5. SEM images of *Bs* spore coating (ATCC#6051) on Pt wires after different biased DC pulses. Parts A, B, and C show the cases after 2, 4, and 7 pulses, respectively. Each DC pulse is set to last 30 s and stop for another 30 s before the next pulse. The enlarged SEM images are inserted which exhibit the different spore deposition densities on the surfaces.

from the surface, a linear relationship between the spore deposits and applied pulse number was found (Figure 6A). By
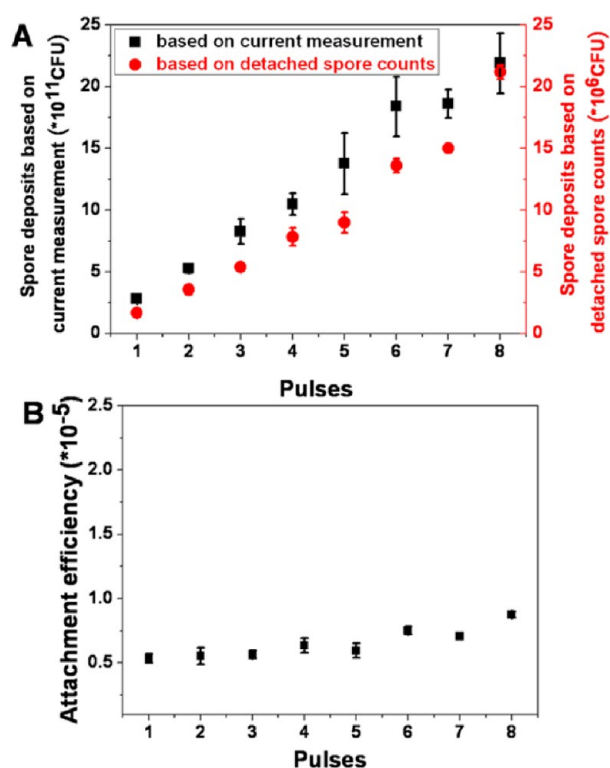
Figure 6. (A) *Bs* spore deposits (ATCC#6051) on the Pt wire after different pulses. The black points are for the spore deposits obtained from the current—time measurement, while the red points are from spore deposits counted from the detached spores. (B) Relationship between spore attachment efficiency and number of pulses for *Bs* spores. The spore attachment efficiency was calculated by the ratio of measured spore deposits (from the detached spore counting), over the idealized spore deposits (from the current—time data). Data were measured four times, which are reflected in the error bars.

our densely packing model (see the Supporting Information and Figure S9), the spore number and number density in one monolayer are 6.1×10^6 and 8×10^{12} m^{-2}, respectively, for *Bs* spores. As are reflected in Figure 6A, these are the spore deposits achieved after four biased pulses (on-time 30 s and off-time 30 s each).

It should be noted that, in this pulsed DC-EPD process up to eight cycles, the pH value of the spore suspension did not vary much (Figure S10, Supporting Information) which had no effect on the deposition rate and spore viability.

4.4. Calculations of the Spore Surface Charge and Deposition Efficiency. In principle, a measurement of the current is also a measure of spore transport to the wire (but not necessarily stick to), if one knows the average charge on a spore. From eq 11, the average charge on a spore can be measured by a prior knowledge of the spore concentration in the suspension and the initial current. A series of initial currents of the spore suspensions were collected under different applied potentials and spore concentrations, which were further subtracted from the initial current of a solution without spores and defined as the effective initial current of spores (I_0) and tabulated in Table 1. The corresponding surface charge (q) per spore is evaluated from eq 11.

However, we still need a relationship between q and q' to determine the fraction of the current associated with the diffuse double layer (Figure S11, Supporting Information). One approach is to find the electrical potential at the shear plane (i.e., the outer radius of solution ions that are carried along with the spore). The Helmholtz—Smoluchowski equation describes the relationship between the shear plane potential (ζ) and the mobility of spores (μ):[63]

$$\mu = \frac{\varepsilon_m}{\eta}\zeta \tag{12}$$

By equating the friction force (eq 5) to the electrophoretic force (eq 2) and also omitting the dielectrophoretic force (eq 3) (note: it has been found that the dielectrophoretic force is much smaller than the electrophoretic force), we can obtain

$$\zeta = \frac{q}{6\pi\varepsilon_m R} \tag{13}$$

In the spherical coordinates, the potential as a function of radial distance from the shear plane can be evaluated, from the simplified Poisson—Boltzmann equation:[63]

$$\zeta = \frac{q}{4\pi\varepsilon_m R_\zeta} \exp(-\kappa R_\zeta) \tag{14}$$

where R_ζ is the radius of the shear plane and κ is the inverse Debye length (1.0384×10^{-6} m^{-1}) in water at room temperature. By combining eqs 13 and 14, we obtain $R_\zeta = 0.35 \times 10^{-6}$ m, thus slightly larger than the radius of one *Bs*

Table 1. Surface Charges and Numbers of Charges for *B. subtilis* Spores (ATCC#6051)^a

concentration (CFU/mL)	voltage (V)	current (mA)	surface charge (C)	number of charges
3.77×10^6	5	0.0002 ± 0.0002	$(5.36 \pm 5.36) \times 10^{-14}$	$(3.35 \pm 3.35) \times 10^5$
8.59×10^7	5	0.0031 ± 0.0008	$(6.20 \pm 0.81) \times 10^{-14}$	$(3.88 \pm 0.51) \times 10^5$
7.67×10^9	5	0.1635 ± 0.0006	$(4.81 \pm 0.01) \times 10^{-14}$	$(3.00 \pm 0.01) \times 10^5$
	10	0.4459 ± 0.0311	$(5.61 \pm 0.20) \times 10^{-14}$	$(3.51 \pm 0.12) \times 10^5$
	20	0.8509 ± 0.1080	$(5.47 \pm 0.35) \times 10^{-14}$	$(3.42 \pm 0.22) \times 10^5$
	30	1.4584 ± 0.2005	$(5.85 \pm 0.40) \times 10^{-14}$	$(3.65 \pm 0.25) \times 10^5$
	40	1.7991 ± 0.2294	$(5.63 \pm 0.36) \times 10^{-14}$	$(3.52 \pm 0.23) \times 10^5$
1.53×10^{10}	5	0.1774 ± 0.0008	$(3.55 \pm 0.01) \times 10^{-14}$	$(2.22 \pm 0.00) \times 10^5$
	10	0.5162 ± 0.0179	$(4.28 \pm 0.07) \times 10^{-14}$	$(2.67 \pm 0.05) \times 10^5$
	20	1.1606 ± 0.0450	$(4.53 \pm 0.09) \times 10^{-14}$	$(2.83 \pm 0.05) \times 10^5$
	30	1.4610 ± 0.1474	$(4.15 \pm 0.21) \times 10^{-14}$	$(2.59 \pm 0.13) \times 10^5$
	50	3.1724 ± 0.2643	$(4.74 \pm 0.20) \times 10^{-14}$	$(2.96 \pm 0.12) \times 10^5$

^{a}Note: the average value of surface charge is 5.01×10^{-14} C, and the average number of charges on the spore surface is 3.13×10^5.

spore (0.336×10^{-6} m). The quantity of charges between R and R_ζ can be calculated:

$$q - q' = -\int_R^{R_\zeta} \rho^* 4\pi r^2 \, dr \tag{15}$$

where ρ^* is the charge density in the diffuse layer which can be expressed from the Poisson equation:[63]

$$\rho^* = (-q)\frac{\kappa^2}{4\pi r}\exp(-\kappa r) \tag{16}$$

Finally, the spore surface charge can be found:

$$q = \frac{q'}{0.9964} \tag{17}$$

Equation 17 implies that the contribution of charges between the spore surface and the shear layer is negligible. Evaluation of eq 11 gives a value of $q = 5.01 \times 10^{-14}$ C. Accordingly, the average number of negative charges on the spore surface is 3.13×10^5 (Table 1). The result above is based on the assumption that the surface charge (or zeta potential) of spores in suspension does not vary during deposition, which is essentially what we observed experimentally (Figure S12, Supporting Information).

The most commonly used method to detect the surface charges of particles is through a measurement of the zeta-potential.[64] The zeta-potential measured for Bs spores yielded values of -33 mV, which accordingly gave a surface charge density of 0.0384 C/m². On the basis of the enlarged SEM images (Figure 3), it is reasonable to assume the spore as a prolate ellipsoid with a semilength axis c and a semiwidth axis a, from which the spore surface area can be estimated. It has been reported that, for Bs spores, $c = 0.535$ μm and $a = 0.24$ μm.[55] Together with the charge density data, the surface charges on the spores can be determined and are listed in Table 2. The

Table 2. Spore Surface Charge Densities, Real Surface Charges, and Number of Charges for B. subtilis Spores (ATCC#6051) from Different Methods

	surface charge density (C/m²)	surface charge (C)	number of charges
zeta-potential method	0.0384	5.36×10^{-14}	3.34×10^5
our method	0.0358	5.01×10^{-14}	3.13×10^5
mobility method[65]	0.0167	2.34×10^{-14}	1.46×10^5

table shows that the charge values obtained from our method and the zeta-potential assay are quite similar. Alternatively, Douglas[65] detected the surface charges of Bs spores through a mobility test in liquid (Table 2). These results suggest that our approach gives results that are consistent with other reported results, with the added benefit of being considerably simpler in terms of the sophistication of the instrumentation needed, and for our purposes the in situ nature of the measurement.

With a known shielded charge q', the net charge accumulation from our current measurement can be directly used to estimate the deposition rate. Accordingly, the deposited spore dose $N_{current}$ on the wire could be determined as (Figure 4)

$$N_{current} = \int_0^t dN_{current} = \frac{1}{q'}\int_0^t I(t) \, dt \tag{18}$$

In our pulsed DC-EPD model, the relationship between spore deposits based on the current measurement and pulses is shown in Figure 6A. $N_{current}$ for just one pulse is in the range of 10^{11} spores, which implies the formation of multiple spore layers. However, one densely packed monolayer of Bs spores (6.1×10^6) actually required four pulses. This leads to a somewhat surprising result that the deposition efficiency is only $\sim 10^{-6}$ (Figure 6B). Thus, it appears that many spores apparently make it to the surface and become dislodged, possibly due to nonvisible gas generation at the electrode.[66] In spite of this low efficiency, the measured deposited spore amount is proportional to the calculated deposits based on the current (Figure 6B), consistent with the results of Hamaker.[67,68] On the basis of this model together with the verification from experiments, our result demonstrates that one is able to in reasonable short deposition time create a near conformal monolayer of spores and subsequently detach them.

5. CONCLUSION

We show in this study the ability to controllably deposit spores electrophoretically to fine wires using a pulsed voltage method which prevents electrolysis. Attached spores can be totally removed by a combination of reversing the electrical polarity and ultrasonicating the wire. We are also able to use this method to quantitatively measure the surface charge on spores and the deposition rate. The method is generic and should be applicable to the deposition of any biological material (e.g., spores, bacteria, viruses) onto metallic surfaces.

■ ASSOCIATED CONTENT

⑤ Supporting Information

Optical microscopic image of Bs spores; optical microscopic images of Bs spores in the continuous and pulsed DC-EPD modes; temporal current in the continuous DC-EPD mode; pH−time relationships during pulsed DC-EPD mode and reversal charging; dense spore packing model on a surface; scheme of the diffuse double layer of the spore surface; zeta potential−pH relationship in spore suspension. This material is available free of charge via the Internet at http://pubs.acs.org.

■ AUTHOR INFORMATION

Corresponding Author

*E-mail: vtlee@umd.edu (V.T.L.); mrz@umd.edu (M.R.Z.).

Notes

The authors declare no competing financial interest.

■ ACKNOWLEDGMENTS

■ REFERENCES

(1) Christopher, G. W.; Cieslak, T. J.; Pavlin, J. A.; Eitzen, E. M. J. Am. Med. Assoc. 1997, 278, 412−417.

(2) Altas, R. M. Annu. Rev. Microbiol. 2002, 56, 167−185.

(3) Grinshpun, S. A.; Adhikari, A.; Li, C.; Reponen, T.; Yermakov, M.; Schoenitz, M.; Dreizin, E.; Trunov, M.; Mohan, S. J. Aerosol Sci. 2010, 41, 352−363.

(4) Gates, S. D.; McCartt, A. D.; Jeffries, J. B.; Hanson, R. K.; Hokama, L. A.; Mortelmans, K. E. J. Appl. Microbiol. 2011, 111, 925−931.

(5) McDonnell, G.; Russell, A. D. *Clin. Microbiol. Rev.* **1999**, *12*, 147−179.

(6) Reddy, N. R.; Tetzloff, R. C.; Solomon, H. M.; Larkin, J. W. *Innovative Food Sci. Emerging Technol.* **2006**, *7*, 169−175.

(7) Staack, N.; Ahrne, L.; Borch, E.; Knorr, D. *J. Food Eng.* **2008**, *89*, 319−324.

(8) Boudam, M. K.; Moisan, M. *J. Phys. D: Appl. Phys.* **2010**, *43*, 295202.

(9) Nicholson, W. L.; Munakata, N.; Horneck, G.; Melosh, H. J.; Setlow, P. *Microbiol. Mol. Biol. Rev.* **2000**, *64*, 548−572.

(10) Setlow, P. *J. Appl. Microbiol.* **2006**, *101*, 514−525.

(11) Setlow, P. *Trends Microbiol.* **2007**, *15*, 172−180.

(12) Gates, S. D.; McCartt, A. D.; Lappas, P.; Jeffries, J. B.; Hanson, R. K.; Hokama, L. A.; Mortelmans, K. E. *J. Appl. Microbiol.* **2010**, *109*, 1591−1598.

(13) McCartt, A. D.; Gates, S. D.; Jeffries, J. B.; Hanson, R. K.; Joubert, L. M.; Buhr, T. L. *Z. Phys. Chem.* **2011**, *225*, 1367−1377.

(14) Grinshpun, S. A.; Li, C.; Adhikari, A.; Yermakov, M.; Reponen, T.; Schoenitz, M.; Dreizin, E.; Hoffmann, V.; Trunov, M. *Aerosol Air Qual. Res.* **2010**, *10*, 414−424.

(15) Zhou, L.; Piekiel, N.; Chowdhury, S.; Zachariah, M. R. *Rapid Commun. Mass Spectrom.* **2009**, *23*, 194−202.

(16) Miller, M. B.; Bassler, B. L. *Annu. Rev. Microbiol.* **2001**, *55*, 165−199.

(17) Mitchell, J. G.; Kogure, K. *FEMS Microbiol. Ecol.* **2006**, *55*, 3−16.

(18) Reguera, G. *Trends Microbiol.* **2011**, *19*, 105−113.

(19) Colville, K.; Tompkins, N.; Rutenberg, A. D.; Jericho, M. H. *Langmuir* **2010**, *26*, 2639−2644.

(20) Fang, B.; Gon, S.; Park, M.-H.; Kumar, K.-N.; Rotello, V. M.; Nusslein, K.; Santore, M. M. *Langmuir* **2012**, *28*, 7803−7810.

(21) Wakeham, A.; Kennedy, R.; McCartney, A. *J. Aerosol Sci.* **2004**, *35*, 835−850.

(22) Lapizco-Encinas, B. H.; Rito-Palomares, M. *Electrophoresis* **2007**, *28*, 4521−4538.

(23) Urdaneta, M.; Smela, E. *J. Micromech. Microeng.* **2008**, *18*, 015001 (8pp).

(24) Markx, G. H.; Dyda, P. A.; Pethig, R. *J. Biotechnol.* **1996**, *51*, 175−180.

(25) Pohl, H. A.; Hawk, I. *Science* **1966**, *152*, 647−649.

(26) Benguigui, L.; Lin, I. J. *J. Electrost.* **1988**, *21*, 205−213.

(27) Huang, Y.; Pethig, R. *Meas. Sci. Technol.* **1991**, *2*, 1142−1146.

(28) Kazoe, Y.; Yoda, M. *Langmuir* **2011**, *27*, 11481−11488.

(29) Douglas, H. W. *Trans. Faraday Soc.* **1955**, *51*, 146−152.

(30) Resnick, M. A.; Tippetts, R. D.; Mortimer, R. K. *Science* **1967**, *158*, 803−804.

(31) Lapizco-Encinas, B. H.; Davalos, R. V.; Simmons, B. A.; Cummings, E. B.; Fintschenko, Y. *J. Microbiol. Methods* **2005**, *62*, 317−326.

(32) Gadish, N.; Voldman, J. *Anal. Chem.* **2006**, *78*, 7870−7876.

(33) Koklu, M.; Park, S.; Pillai, S. D.; Beskok, A. *Biomicrofluidics* **2010**, *4*, 034107.

(34) Chen, G.; Driks, A.; Tawfiq, K.; Mallozzi, M.; Patil, S. *Colloids Surf., B* **2010**, *76*, 512−518.

(35) Seale, R. B.; Bremer, P. J.; Flint, S. H.; McQuillan, A. J. *J. Appl. Microbiol.* **2010**, *109*, 1339−1348.

(36) Poortinga, A. T.; Busscher, H. J. *Biotechnol. Bioeng.* **2000**, *67*, 117−120.

(37) Neirinck, B.; Van Mellaert, L.; Fransaer, J.; Van der Biest, O.; Anne, J.; Vleugels, J. *Electrochem. Commun.* **2009**, *11*, 1842−1845.

(38) Novak, S.; Maver, U.; Peternel, S.; Venturini, P.; Bele, M.; Gaberscek, M. *Colloid Surface A* **2009**, *340*, 155−160.

(39) Ammam, M.; Fransaer, J. *Electrochim. Acta* **2010**, *55*, 3206−3212.

(40) Hsu, P.-C.; Seol, S.-K.; Lo, T.-N.; Liu, C.-J.; Wang, C.-L.; Lin, C.-S.; Hwu, Y.; Chen, C. H.; Chang, L.-W.; Je, J. H.; Margaritondo, G. *J. Electrochem. Soc.* **2008**, *155*, D400−D407.

(41) Craig, V. S. J. *Soft Matter* **2011**, *7*, 40−48.

(42) Tauveron, G.; Slomianny, C.; Henry, C.; Faille, C. *Int. J. Food Microbiol.* **2006**, *110*, 254−262.

(43) Mercier-Bonin, M.; Dehouche, A.; Morchain, J.; Schmitz, P. *Int. J. Food Microbiol.* **2011**, *146*, 182−191.

(44) Granhag, L. M.; Finlay, J. A.; Jonsson, P. R.; Callow, J. A.; Callow, M. E. *Biofouling* **2004**, *20*, 117−122.

(45) Bower, C. K.; McGuire, J.; Daeschel, M. A. *Trends Food Sci. Technol.* **1996**, *7*, 152−157.

(46) Andersson, A.; Ronner, U. *Biofouling* **1998**, *13*, 51−67.

(47) Amman, M.; Fransaer, J. *Biosens. Bioelectron.* **2009**, *25*, 191−197.

(48) Neirinck, B.; Fransaer, J.; Van der Biest, O.; Vleugels, J. *Electrochem. Commun.* **2009**, *11*, 57−60.

(49) Besra, L.; Uchikoshi, T.; Suzuki, T. S.; Sakka, Y. *J. Am. Ceram. Soc.* **2008**, *91*, 3154−3159.

(50) Besra, L.; Uchikoshi, T.; Suzuki, T. S.; Sakka, Y. *J. Eur. Ceram. Soc.* **2009**, *29*, 1837−1845.

(51) Poortinga, A. T.; Bos, R.; Norde, W.; Busscher, H. J. *Surf. Sci. Rep.* **2002**, *47*, 1−32.

(52) Chung, E.; Yiacoumi, S.; Lee, I.; Tsouris, C. *Environ. Sci. Technol.* **2010**, *44*, 6209−6214.

(53) Walton, O. R. *KONA* **2008**, *26*, 129−141.

(54) Srivastava, S. K.; Gencoglu, A.; Minerick, A. R. *Anal. Bioanal. Chem.* **2011**, *399*, 301−321.

(55) Carrera, M.; Zandomeni, R. O.; Fitzgibbon, J.; Sagripanti, J.-L. *J. Appl. Microbiol.* **2007**, *102*, 303−312.

(56) Ristenpart, W. D.; Aksay, I. A.; Saville, D. A. *Langmuir* **2007**, *23*, 4071−4080.

(57) Ristenpart, W. D.; Aksay, I. A.; Saville, D. A. *J. Fluid Mech.* **2007**, *575*, 83−109.

(58) Atkins, P. *Physical Chemistry*, 6th ed.; W. H. Freeman and Company: New York, 1997.

(59) Burgos, J.; Ordonez, J. A.; Sala, F. *Appl. Microbiol.* **1972**, *24*, 497−498.

(60) Ordonez, J. A.; Burgos, J. *Appl. Environ. Microbiol.* **1976**, *32*, 183−184.

(61) Pagan, R.; Esplugas, S.; Gongora-Nieto, M. M.; Barbosa-Canovas, G. V.; Swanson, B. G. *Food Sci. Technol. Int.* **1998**, *4*, 33−44.

(62) Spilimbergo, S.; Dehghani, F.; Bertucco, A.; Foster, N. R. *Biotechnol. Bioeng.* **2003**, *82*, 118−125.

(63) Hiemenz, P. C.; Rajagopalan, R. *Principles of Colloid and Surface Chemistry*, 3rd ed.; Taylor & Francis Group: Boca Raton, FL, 1997.

(64) Tsai, D.-H.; Pease, L. F., III; Zangmeister, R. A.; Tarlov, M. J.; Zachariah, M. R. *Langmuir* **2009**, *25*, 140−146.

(65) Douglas, H. W. *Trans. Faraday Soc.* **1959**, *55*, 850−856.

(66) Bohmer, M. *Langmuir* **1996**, *12*, 5747−5750.

(67) Hamaker, H. C. *Trans. Faraday Soc.* **1940**, *36*, 279−87.

(68) Sarkar, P.; Nicholson, P. S. *J. Am. Ceram. Soc.* **1996**, *79*, 1987−2002.